Optimal Coupling of LED Sources to Optical Fibers

Ching-Long Jiang
AMP Incorporated

ABSTRACT

A novel ray tracing model is described for analyzing coupling of a spherically surfaced LED to a flat-ended fiber using a TO can with a sapphire cap, Salient features of the model are (1) closed form solution of the trajectories of all rays being coupled into the fiber, (2) inclusion of large-angle rays in the model calculation, and (3) calculation of the transmitted power through each interface. The coupling efficiency is defined as the ratio of the power coupled into a fiber to the power generated in the LED. The maximum efficiency of 10 percent calculated by this model is verified experimentally.

INTRODUCTION

Two types of light sources are considered most widely used for fiberoptic communications: semiconductor lasers and light-emitting diodes (LEDs). Advantages of LEDs are high reliability, low cost, and small temperature dependence of the radiative power. A disadvantage is that in conventional designs the power coupled from an LED into an optical fiber is usually less than that from a laser. Therefore, for each specific design the coupling efficiency of the LED into the fiber must be optimized in addition to improving the external quantum efficiency of the LED.

The coupling efficiency is defined as the ratio of the power coupled into an optical fiber to the power emitted by the light source. Because of the small size of the emitting area of a laser or edge-emitting LED, the common methods of analyzing the degree of coupling assume infinitesimal light sources.

For an LED with a finite emitting area, the coupling efficiency has been analyzed for a specific arrangement by Deimal.[1] He developed a ray-tracing program for LEDs with iridium phosphide (InP) lenses that yields the power in arbitrary units coupled into a 50-μm core fiber without the sapphire collimating lens. In this particular case maximum power coupling required a distance between the apex of the InP lens and the center of the fiber of 10 to 30 μm. Such a short distance is quite appropriate for a pigtailed fiber geometry but not for LEDs packaged in TO cans. Another major shortcoming of Deimal's model is the rather long computation time inherent in the mathematical approach chosen. The active area of a radius of 30 **m**m is divided into 707 elements of 4 μm^2, the InP lens is divided into 5539 elements of the same size. The ray tracing connects each of the 707 small segments of the active area to each of the 5539 small segments of the InP lens. The permutational nature of this approach results in many more rays being traced than necessary. If the number of rays calculated were proportional to the Lambertian distribution, the computation time could be reduced.

The method reported in this paper assumes that the number of rays being generated at the active area is proportional to the Lambertian distribution. Each ray passes through the InP lens and the sapphire sphere into the fiber. The amount of light coupled into the fiber depends on a number of variables. The following additional assumptions are used in this paper:

1. uniform light intensity distribution in the emitting area
2. perfectly spherical InP lens
3. perfect sapphire sphere as the cap in the TO can
4. a step index fiber with core diameter of 62.5 μm

Variables include the wafer thickness, i.e., the distance of the center of the emitting area from the apex of the lens, the radius of curvature of the lens, axial and lateral displacement of the sapphire sphere, axial and lateral displacement of the fiber, and the radius of the sapphire sphere.

MODELING

The ray-tracing model has been divided into five sections corresponding to each optical element.

Section 1: Light-Emitting Area

The (x, y) plane is placed coplanar with the light-emitting area of the LED and the origin of the global coordinate system is chosen to be the center of this area as shown in Figure 1. The total light-emitting area with a radius of R0 is divided into infinitesimal segments, each of them carrying the coordinates (x_1, y_1, z_1) with Z = 0. The light emits from each of these infinitesimal elements under the direction cosines (L_1, M_1, N_1) as shown in Figure 1.

$$L_1 = \cos\phi \cdot \sin\theta$$
$$M_1 = \mathrm{sim}\,\phi \cdot \sin\theta$$
$$N_1 = \cos\theta$$

Because of the assumption of a Lambertian source, the number of rays per solid angle emitted from each element is proportional to $\cos\theta$.

Section 2: The InP Lens

Because of the similarity of the algorithms required in Sections 3 and 4 with those introduced in the present section, Section 2, the equations in this section are written in a generalized form in terms of i. It is i = 1 in Section 2, i = 2 in Section 3, and i = 4 in Section 4.

A spherical InP lens with radius R_i is centered at (X_i, Y_i, Z_i). Assuming a ray emitted by the surface element at (x_i, y_i, z_i) with direction cosines (L_i, M_i, N_i) meets the InP lens at $(x_{i+1}, y_{i+1}, z_{i+1})$, then $(x_{i+1}, y_{i+1}, z_{i+1})$ must satisfy the following equations:

$$x_{i+1} = x_i + (z_{i+1} - z_i) \cdot \frac{L_i}{N_i} \qquad (1)$$

$$y_{i+1} = y_i + (z_{i+1} - z_i) \cdot \frac{M_i}{N_i} \qquad (2)$$

$$(x_{i+1} - X_i)^2 + (y_{i+1} - Y_i)^2 + (z_{i+1} - Z_i)^2 - R_i^2 = 0 \qquad (3)$$

By substituting Equations 1 and 2 into Equation 3, we obtain a quadratic equation

$$A_i \cdot z_{i+1}^2 + B_i \cdot z_{i+1} + C_i = 0 \qquad (4)$$

where

$$A_i = 1/N_i^2$$
$$B_i = D_i + 2(1 - A_i) - 2Z_i$$
$$C_i = (A_i - 1)z_i^2 + Z_i^2 + (x_i - X_i)^2 + (y_i - Y_i)^2 - R_i^2 - D_i z_i$$
$$D_i = 2(x_i - X_i)L_i/N_i + 2(y_i - Y_i)M_i/N_i.$$

Then it is

$$z_{i+1} = \frac{-B_i \pm \sqrt{B_i^2 - 4 \cdot A_i \cdot C_i}}{2 \cdot A_i} \qquad (5)$$

and x_{i+1} and y_{i+1} are found from Equations 1 and 2.

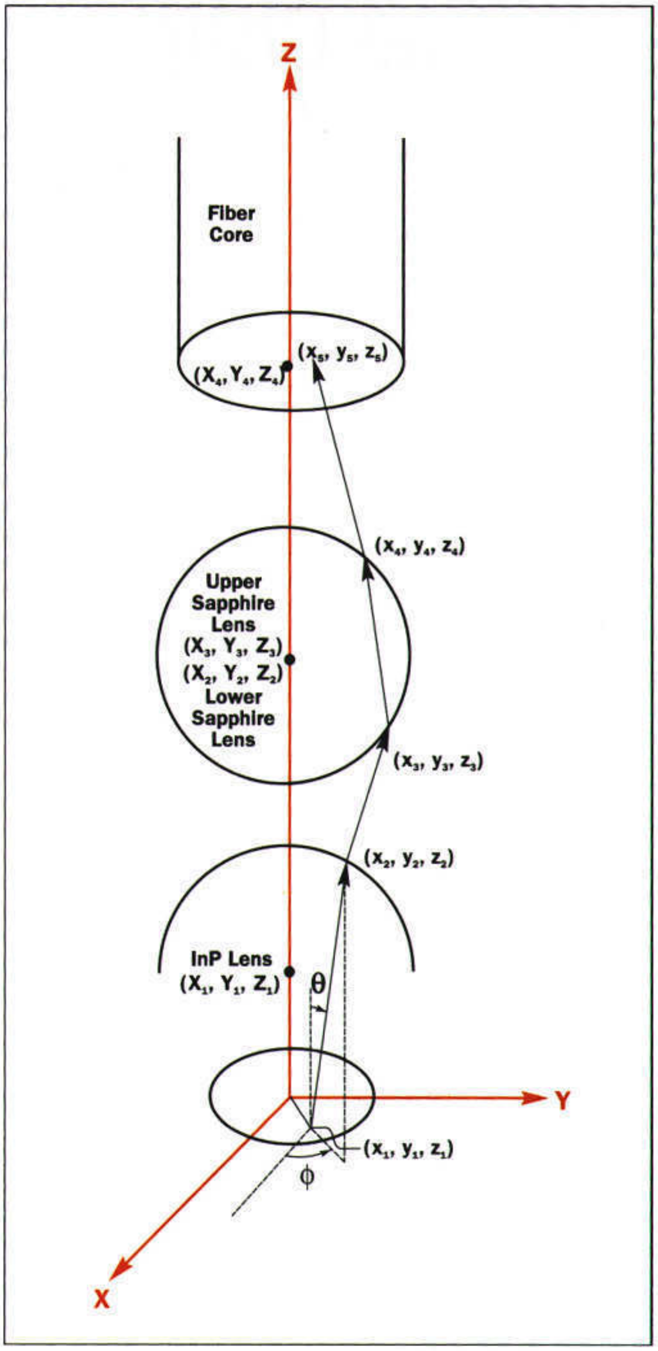

Figure 1. Schematic of the global coordinate system and interfaces used in the ray-tracing model.

The InP lens is located on the positive side of the z-axis. Therefore, the positive sign is chosen in front of square root in this section. If

$$B_i^2 - 4A_i^*C_i < 0,$$

there is no solution, which means that the ray does not meet the InP lens and would not be coupled into the fiber.

The distance the light ray travels inside the InP material is

$$S = \sqrt{(x_{i+1} - x_i)^2 + (y_{i+1} - y_i)^2 + (z_{i+1} - z_i)^2}$$

For a known absorption coefficient ψ, the transmitted light power that reaches the interface has to be multiplied by an absorption factor Ψ.

$$\Psi = e^{-\psi S}$$

From Equation 3, the unit vector $\mathbf{n}(\alpha_i, \beta_i, \gamma_i)$ along the normal at point $(x_{i+1}, y_{i+1}, z_{i+1})$ on the surface can be expressed as

$$\alpha_i = (x_{i+1} - X_i)/R_i \tag{6}$$

$$\beta_i = (y_{i+1} - Y_i)/R_i \tag{7}$$

$$\gamma_i = (z_{i+1} - Z_i)/R_i \tag{8}$$

To determine the direction cosines $r_{i+1}(L_{i+1}, M_{i+1}, N_{i+1})$ of the refracted ray, Snell's law is written in vector form

$$n_{i+1}(\mathbf{r_{i+1}} \wedge \mathbf{n}) = n_i(\mathbf{r_i} \wedge \mathbf{n}), \tag{9}$$

where $\mathbf{n}$ is a unit vector parallel to the normal at the point of incidence $(x_{i+1}, y_{i+1}, z_{i+1})$, n_i and n_{i+1} are the refraction indices of material i and i + 1, and $\mathbf{r_i}$ and $\mathbf{r_{i+1}}$ are unit vectors along the incident and refracted rays. The equation can be multiplied vectorially by $\mathbf{n}$ to obtain

$$n_{i+1}(\mathbf{r}_{i+1} - \mathbf{n}(\mathbf{r}_{i+1} \cdot \mathbf{n})) = n_i(\mathbf{r_i} - \mathbf{n}(\mathbf{r_i} \cdot \mathbf{n})).$$

This can be expanded in scalar form by setting (L_i, M_i, N_i), $(L_{i+1}, M_{i+1}, N_{i+1})$, and $(\alpha_i, \beta_i, \gamma_i)$ as the components r_i, r_{i+1} and $\mathbf{n}$ respectively, so that these quantities are direction cosines, yielding

$$n_{i+1}L_{i+1} - n_iL_i = k_i\alpha_i \tag{10}$$

$$n_{i+1}M_{i+1} - n_iM_i = k_i\beta_i \tag{11}$$

$$n_{i+1}N_{i+1} - n_iN_i = k_i\gamma_i \tag{12}$$

where

$$\begin{aligned} k_i &= n_{i+1}(\mathbf{r_{i+1}} \cdot \mathbf{n}) - n_i(\mathbf{r_i} \cdot \mathbf{n}) \\ &= n_{i+1}\cos I_{i+1} - n_i \cos I_i \\ &= \{E_i\}^{1/2} - n_i \cos I_i \end{aligned} \tag{13}$$

$$\begin{aligned} E_i &= n_{i+1}^2 - n_i^2(1 - \cos^2 I_i) \\ \cos I_i &= \alpha_i L_i + \beta_i M_i + \gamma_i N_i \\ \cos I_{i+1} &= \alpha_i L_{i+1} + \beta_i M_{i+1} + \gamma_i N_{i+1} \end{aligned} \tag{14}$$

and I_i and I_{i+1} are the angles of incidence and refraction. If $E_i < 0$, then k_i becomes imaginary, indicating total internal reflection inside the InP lens. Formulation of the ray-tracing procedure can also be found in Reference 2.

To calculate the power transmitted through the interface, the incoming power has to be multiplied by the transmissivity τ_i.

$$\tau_i = \frac{n_{i+1} \cdot \cos I_{i+1}}{n_i \cdot \cos I_i} \cdot \frac{T^2}{A^2} \tag{15}$$

The relationship between the amplitudes of the incoming fields A and transmitted fields T is

$$T_\perp = \frac{2 \cdot n_i \cdot \cos I_i}{n_i \cdot \cos I_i + n_{i+1} \cdot \cos I_{i+1}} \cdot A_\perp$$

$$T_\parallel = \frac{2 \cdot n_i \cdot \cos I_i}{n_{i+1} \cdot \cos I_i + n_i \cdot \cos I_{i+1}} \cdot A_\parallel$$

where $T_\perp$ and $T_\parallel$ stand for the amplitudes of the transmitted field polarized perpendicular and parallel relative to the plane of incidence; Correspondingly, $A_\perp$ and $A_\parallel$ represent the amplitudes of the incoming fields. It is for both fields

$$T^2 = T_\perp^2 + T_\parallel^2$$

$$A^2 = A_\perp^2 + A_\parallel^2$$

Since LEDs are unpolarized sources, $T_\perp = T_\parallel$ and $A_\perp = A_\parallel$. As a ray passes through the InP-air interface, partial polarization of the incoming unpolarized beam occurs, and each component, i.e., perpendicular and parallel to the plane of incidence on the lens surface, has to be treated separately at every interface. L_{i+1}, M_{i+1}, N_{i+1} could be obtained from Equations 10, 11, and 12 as follows:

$$L_{i+1} = (n_iL_i + k_i\alpha_i)/n_{i+1} \tag{16}$$

$$M_{i+1} = (n_iM_i + k_i\beta_i)/n_{i+1} \tag{17}$$

$$N_{i+1} = (n_iN_i + k_i\gamma_i)/n_{i+1} \tag{18}$$

Equations 16, 17, and 18 are also suitable for tracing skew rays. Both large and small angle rays are being included in this calculation without any approximation.

Section 3: Lower Half of Sapphire Lens

The equations of this section are identical to the equations of Section 2 except that now i = 2. The negative sign in Equation 5 is chosen in this section versus the positive sign chosen in Section 2. The solutions in the lower half of the sapphire lens have the negative sign in Equation 5. Due to the techniques used in brazing and metallizing the sapphire sphere to the TO can, the metallization on the sapphire lens blocks some of the light rays. Considering a worst case, the specifications of the TO can manufacturer should be used as criteria for calculating the number of rays being accepted into the sapphire sphere. Usually, TO can manufacturers issue a minimum specification (RR2) for the aperture of the lower half of the sapphire lens. Therefore, if it is

$$z_3 < (Z_2 - \sqrt{R_2^2 - RR2^2})$$

the light ray will be accepted into the lower half of the sapphire lens.

Section 4: Upper Half of Sapphire Lens

The equations in this section are identical to those in Section 2 except that now i = 3. The solutions in the upper half of the sapphire lens require the positive sign in Equation 5. Assuming RR3 as the minimum aperture for the upper half of the sapphire lens, then

$$\text{if } z_4 > Z_3 + \sqrt{R_3^2 - RR3^2},$$

the light ray will pass through its upper half.

Section 5: Fiber

The fiber is described here using the following characteristics: refractive index, n_5; numerical aperture, NA; core radius, RF; location of the center of fiber core, (X_4, Y_4, Z_4); unit vector along the normal at point (X_4, Y_4, Z_4) of fiber core, $\mathbf{n}(\alpha_4, \beta_4, \gamma_4)$. The following two equations describe the ray leaving the sapphire lens from (x_4, y_4, z_4) with direction cosines (L_4, M_4, N_4):

$$x = x_4 + L_4(z - z_4)/N_4$$

$$y = y_4 + M_4(z - z_4)/N_4$$

The center of the fiber core is located in the plane z = Z4 parallel to the (x, y) plane where the x and y have the following values:

$$x_5 = x_4 + L_4(z_5 - z_4)/N_4$$

$$y_5 = y_4 + M_4(z_5 - z_4)/N_4$$

with

$$z_5 = Z_4.$$

If the ray is accepted into the core of the fiber, then the following condition must be satisfied:

$$(x_5 - X_4)^2 + (y_5 - Y_4)^2 < RF^2.$$

In addition, there is a condition for the light ray to remain inside the core of the fiber. This requires that the angle of incidence into the fiber has to be less than the numerical aperture.[3] After some arithmetic, this condition can be expressed as

$$N_4 > \sqrt{1 - NA^2}$$

Only rays meeting both conditions will be counted as being accepted into the fiber. Calculation of the transmissivity τ_4 is the same as that in Equation 15 in Section 2 except for i = 4.

The concepts described above were realized by using a computer program written in FORTRAN. The program counts the number of light rays accepted into the fiber, tabulates the number of light rays rejected at each stage, and calculates the total power according to the equations introduced for transmissivities at each interface and for absorption inside the corresponding optical elements. Because none of the common approximations were introduced, the model approaches reality. In particular it includes the frequently suppressed large-angle rays.

Coupling efficiency is defined as the ratio of the power launched into a fiber to the optical power generated by the LED. In designing an LED package, all parameters entering the model can be varied to identify combinations that would yield optimized coupling efficiency. Prior to building experimental samples, the ray-tracing model described here can be used to predict coupling efficiency and, thus, becomes a powerful tool for LED package design.

RESULTS AND DISCUSSION

The accuracy of this model depends on the number of elements of equal size chosen for dividing the active area. However, there is a trade-off between the accuracy determined by the segmentation and computation time. If one chooses the accuracy for a coupling efficiency higher than 1 percent to be ±0.1 percent, then 400 emitting points with equally divided active areas and 400 rays from each emitting point with Lambertian distribution are required. The accuracies in coupling efficiency between 400 × 400 and 1600 × 1600 is better than 0.1 percent. Therefore, the calculation below is based on the 400 rays from 400 emitting points with equally divided active areas.

This model allows for a great deal of flexibility in the choice of values for each needed parameter. The values in Table 1 were chosen as an example in calculating the coupling efficiency.

The highest coupling efficiency of 10 percent was obtained with the variable values shown in Table 2. This highest coupling efficiency of 10 percent was verified experimentally.[4] Figure 2 was obtained by plotting the coupling efficiency as a function of X_4 and Y_4 with the above parameters. It is very useful for illustrating the profile of the coupling efficiency as a function of X_4 and Y_4. Figure 2 also shows the drop of the coupling efficiency if the fiber is not aligned perfectly. Figure 3 is a contour plot of Figure 2 and shows that the coupling efficiency is reduced from 10 percent to 8 percent if the fiber is misaligned by 25 µm. The coupling efficiency is reduced further to less than 1 percent if the misalignment of the fiber increases to 75 µm. As Figure 3 illustrates, the coupling efficiency varies substantially with misalignment. Therefore, the light output power from the fiber would also be expected to drop substantially, which is undesirable.

Table 1.

	Description	Value
n_1	index of refraction of Indium Phosphide	3.2
n_2	index of refraction of air	1.0
n_3	index of refraction of sapphire	1.75
n_4	index of refraction of air	1.0
n_5	index of refraction of fiber	1.4719
ψ	absorption coefficient of Indium Phosphide[1]	0.12/mm
R0	radius of LED light emitting area	12 µm
R_2	radius of lower half of sapphire lens	635 µm
R_3	radius of upper half of sapphire lens	635 µm
RR2	radius of aperture on the lower sapphire lens	419 µm
RR3	radius of aperture on the upper sapphire lens	419 µm
RF	core radius of fiber	31.25 µm
NA	numerical aperture of fiber	0.275

Table 2.

	Description	Value (µm)
X_1	x-coordinate of the center of InP lens	0
Y_1	y-coordinate of the center of InP lens	0
Z_1	z-coordinate of the center of InP lens	20
R_1	radius of InP lens	124
X_2	x-coordinate of the lower sapphire lens	0
Y_2	y-coordinate of the lower sapphire lens	0
Z_2	z-coordinate of the lower sapphire lens	1478
X_3	x-coordinate of the upper sapphire lens	0
Y_3	y-coordinate of the upper sapphire lens	0
Z_3	z-coordinate of the upper sapphire lens	1478
X_4	x-coordinate of the center of fiber tip	0
Y_4	y-coordinate of the center of fiber tip	0
Z_4	z-coordinate of the center of fiber tip	2713

Table 3.

	Description	Value
Z_2	z-coordinate of the lower sapphire lens	1168 µm
Z_3	z-coordinate of the upper sapphire lens	1168 µm
Z_4	z-coordinate of the center of fiber tip	2896 µm

A second example was prepared for a different configuration by modifying the three parameters listed in Table 3. All others are the same as before.

The results are shown in Figure 4. In this example the coupling efficiency remains fairly constant on the plateau area and the amount of light coupled into the fiber becomes more uniform. Figure 5 is a contour plot of Figure 4. The area with 5 percent coupling efficiency in Figure 5 is

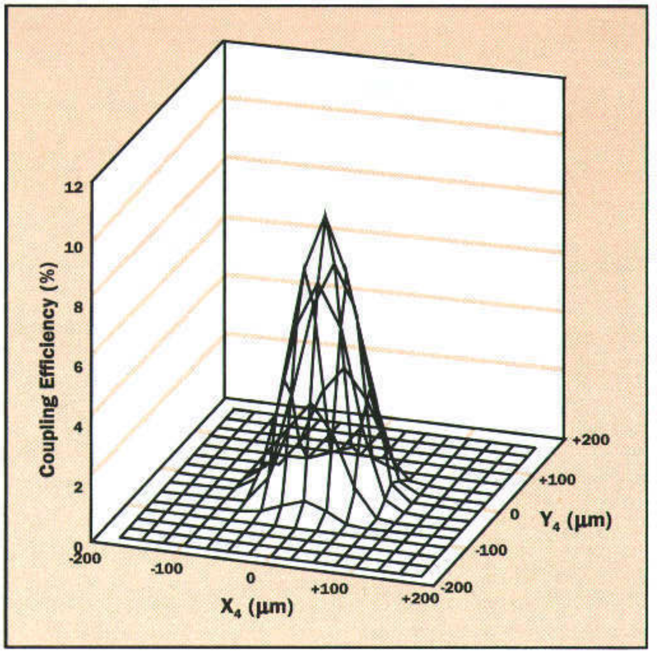

Figure 2. The surface profile plot of the coupling efficiency as a function of the center of fiber core position (X_4, Y_4) at Z_4 = 2713 µm plane.

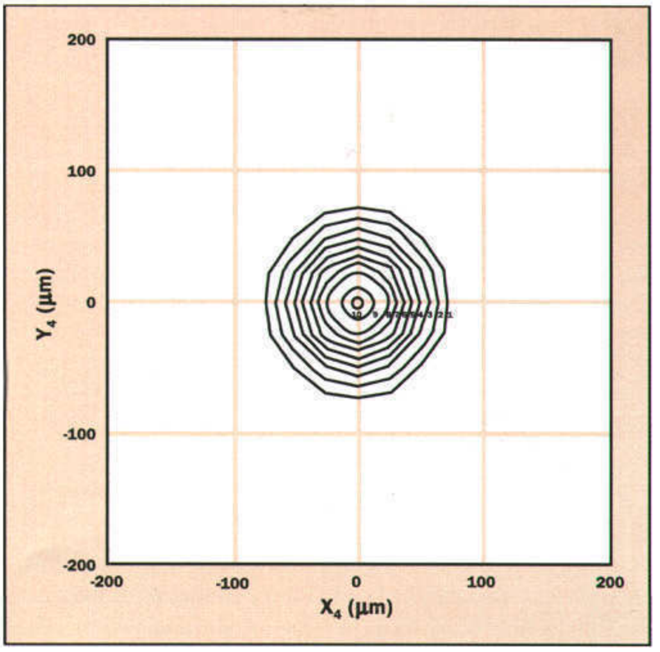

Figure 3. The contour plot of the coupling efficiency as a function of the center of fiber core position (X_4, Y_4) at Z_4 = 2713 µm plane.

larger than the area with 5 percent coupling efficiency in Figure 3 obtained for the first combination of parameters. Therefore, the second configuration is more suitable for manufacturing than the first configuration.

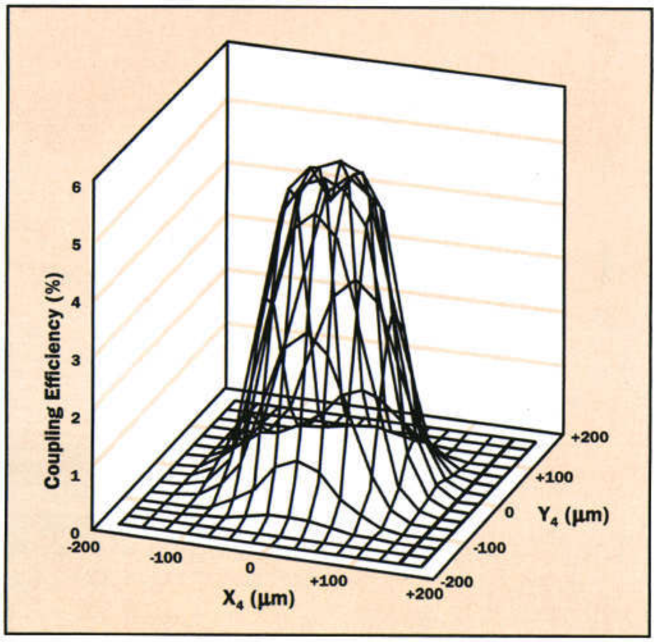

Figure 4. The surface profile plot of the coupling efficiency as a function of the center of fiber core location (X_4, Y_4) at Z_4= 2896 µm plane.

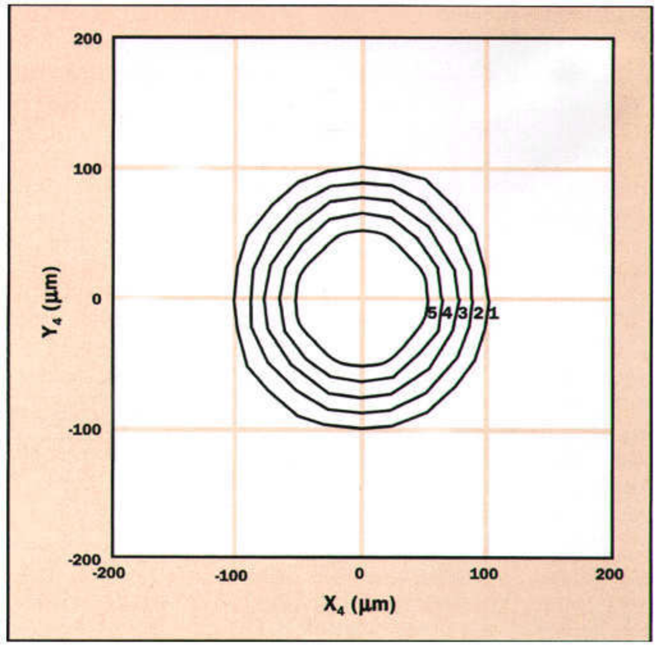

Figure 5. The contour plot of the coupling efficiency as a function of the center of fiber core position (X_4, Y_4) at Z_4= 2896 µm plane.

SUMMARY

Depending on the specified tolerance and power requirements, the model presented is a powerful tool for designing LED packages. This is illustrated on two specific examples. If very precise fiber positioning is possible, the configuration of the first example would offer itself to achieve high coupling efficiency. If the tight tolerance of the fiber placement assumed for the first example cannot be met, then the second configuration would allow for uniform light output power from LED package.

ACKNOWLEDGMENTS

The author thanks A. Heiney for providing the experimental data to verify the theoretical calculation in this paper, R. Wilson for providing the past experience in building this ray-tracing model, J. Kulick and E. Imhoff for their continuous encouragement, and M. Mashas for his critical reading of this manuscript.

REFERENCES

1. P.P. Deimel, "Calculations for integral lenses on surface-emitting diodes,'' *Applied Optics* **24** (3), 343 (1985).

2. W.T. Welford and R. Winston, "High Collection Non-imaging Optics" in Some *Basic Ideas in Geometrical Optics* (Academic Press, San Diego, CA 1989), pp. 10-13.

3. K.A. Jones, *Introduction to Optical Electronics* (Harper & Row, New York, 1987), p.67.

4. Allan Heiney, AMP (private communication).

Ching-Long Jiang is a member of the technical staff at the Lytel Division, AMP Incorporated.

He was born in Keelung, Taiwan. He received the B.S. degree in physics from Fu Jen Catholic University, Taiwan in 1970, the M.S. and Ph.D. degrees in physics from the University of California, Riverside in 1974 and 1979, respectively. In 1979 he joined Southern Methodist University at Dallas, Texas where his work was concerned with the research and development of low cost polycrystalline solar cells. In 1982, he joined Rockwell International where his research and development activities were the design, fabrication and characterization of long-wavelength semiconductor lasers and detectors for lightwave communication. Since joining Lytel Division, AMP Incorporated in 1992, his research interest has expanded into the area of high efficient light coupling between optical devices and fibers.